AIP | Applied Physics Letters

Ultraviolet optical near-fields of microspheres imprinted in phase change films

J. Siegel, D. Puerto, J. Solis, F. J. García de Abajo, C. N. Afonso et al.

Citation: Appl. Phys. Lett. 96, 193108 (2010); doi: 10.1063/1.3428582
View online: http://dx.doi.org/10.1063/1.3428582
View Table of Contents: http://apl.aip.org/resource/1/APPLAB/v96/i19
Published by the American Institute of Physics.

Related Articles

Role of measurement voltage on hysteresis loop shape in Piezoresponse Force Microscopy
Appl. Phys. Lett. 101, 192902 (2012)

Minimum domain size and stability in carbon nanotube-ferroelectric devices
Appl. Phys. Lett. 101, 142906 (2012)

Crystallographic direction dependence of direct current field induced strain and phase transitions in Na0.5Bi0.5TiO3-x%BaTiO3 single crystals near the morphotropic phase boundary
Appl. Phys. Lett. 101, 141912 (2012)

Enhanced piezoelectric and antiferroelectric properties of high-TC perovskite of Zr-substituted Bi(Mg1/2Ti1/2)O3-PbTiO3
J. Appl. Phys. 112, 074101 (2012)

Pinned interface dipole-induced tunneling electroresistance in ferroelectric tunnel junctions: A theoretical investigation
J. Appl. Phys. 112, 054104 (2012)

Additional information on Appl. Phys. Lett.

Journal Homepage: http://apl.aip.org/
Journal Information: http://apl.aip.org/about/about_the_journal
Top downloads: http://apl.aip.org/features/most_downloaded
Information for Authors: http://apl.aip.org/authors

ADVERTISEMENT

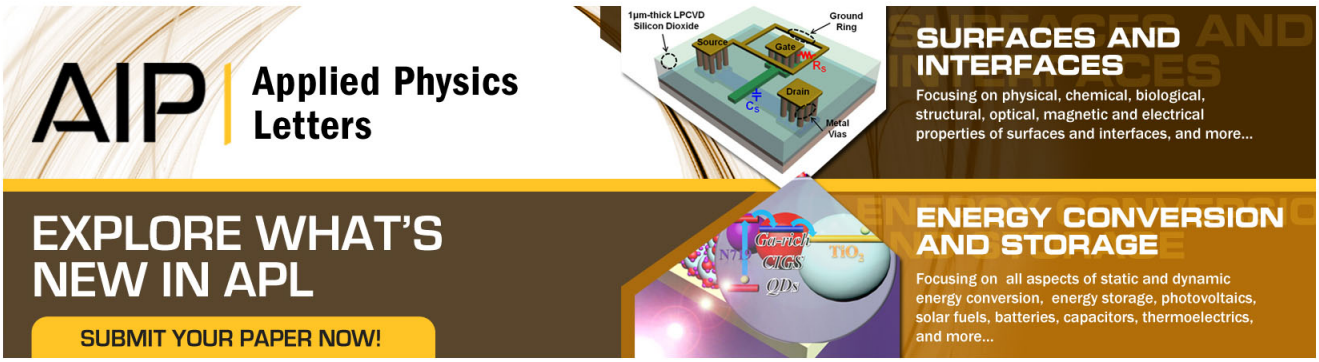

Ultraviolet optical near-fields of microspheres imprinted in phase change films

J. Siegel,[1,a)] D. Puerto,[1] J. Solis,[1] F. J. García de Abajo,[1] C. N. Afonso,[1] M. Longo,[2] C. Wiemer,[2] M. Fanciulli,[2] P. Kühler,[3] M. Mosbacher,[3] and P. Leiderer[3]
[1]*Instituto de Optica, CSIC, Serrano 121, 28006-Madrid, Spain*
[2]*MDM National Laboratory, CNR-INFM, Via C. Olivetti 2, 20041 Agrate Brianza, Italy*
[3]*Faculty of Physics, University of Konstanz, Universitätsstraße 10, 78457 Konstanz, Germany*

(Received 26 February 2010; accepted 17 April 2010; published online 12 May 2010)

We report an experimental method for directly imaging optical near-fields of dielectric microspheres upon illumination with ultraviolet nanosecond laser pulses. The intensity distribution is imprinted in chalcogenide films leaving behind a characteristic fingerprint with features below 200 nm in size, which we read out with high-resolution field emission scanning electron microscopy. The experimental results are well matched by a rigorous solution of Maxwell's equations. Compared to previous works using infrared femtosecond laser pulses, the use of ultraviolet nanosecond pulses is identified to be superior in terms of minimum recordable features size and surface roughness of the imprint. © *2010 American Institute of Physics*. [doi:10.1063/1.3428582]

Light interacting with a small particle gives rise to a complex three-dimensional (3D) optical near-field (ONF) surrounding the object, which depends on the properties of the light, the scattering particle, and the supporting substrate. While the ONF is a pillar stone of microscopy at the submicron scale,[1] the strong field enhancement at the substrate surface makes it also an exciting approach for material processing. Employing femtosecond (fs) laser pulses, this field enhancement is sufficient to produce local ablation at a substrate underneath dielectric microspheres, yielding nanopits with diameters below the diffraction limit.[2] This discovery has led to a widespread activity by many groups in order to exploit this effect for nanopatterning.[3–6]

Despite the huge progress in achieving controlled nanostructuring of surfaces, a main challenge still has to be met. High-precision nanostructuring based on ONFs requires a detailed knowledge of the complex two-dimensional 2D near-field intensity distribution at the substrate plane. Specific methods devised to image near fields [e.g., far-field optical microscopy (OM), near-field scanning OM, and photoelectron microscopy] have limited spatial resolution either due to the diffraction limit or the size of the scanning probe. A method free from this limitation is near-field ablation using fs laser pulses, in which the intensity distribution is translated into a topographic distribution. While this strategy is capable to reveal fine structures of ONFs,[7] it only yields qualitative images, since it exploits nonlinear absorption and ablation to produce the imprint, thus distorting the actual ONF distribution. A different method, free from these drawbacks, has recently been reported for the specific case of fs laser pulses at 800 nm.[8] It is based on the use of thin chalcogenide films, used in rewritable optical disks due to their ability to switch between a highly reflective, crystalline, and a less reflective, amorphous phase upon exposure to pulsed laser radiation.[9] This material has also been used very recently to demonstrate parallel nanolithography for nanodevice fabrication employing microlens arrays and wet etching.[10] When using it for imaging ONFs, their corresponding 2D intensity distribution is mapped onto a pattern of well-defined amorphous and crystalline regions, only involving linear absorption and no ablation. The pattern can be read-out with a conventional optical microscope and is directly linked to the near-field intensity distribution.[8]

In the present work, we report imprinting of much smaller patterns than those reported in Ref. 8 by using ultraviolet (UV) light at 193 nm. This corroborates the applicability of our method to patterning in the nanoscale. While UV wavelengths are optimum for imprinting nanometer-scale features, the read-out of these small features proves problematic with the strategy used in Ref. 8 because of the limited spatial resolution of OM. The beauty of the concept of using chalcogenide films to image ONFs is the range of different contrast types that can be exploited for read-out. In addition to a considerable optical contrast between the amorphous and the crystalline phase,[11] which was exploited in Ref. 8, the material features an enormous contrast in electrical resistivity,[12] as well as a considerable topographical contrast.[13] Accordingly, we introduce in the present work scanning electron microscopy (SEM) to probe the resulting patterns, and we demonstrate that this is a suitable, high-resolution read-out method for these patterns.

Samples were prepared as in Ref. 8, using as substrates sputter-deposited 40-nm-thick, fcc polycrystalline $Ge_2Sb_2Te_5$ (GST) films on Si [001] wafers covered by a 10-nm-thick amorphous SiO_2 buffer layer, custom-produced by Numonyx, Italy. Two sizes of spherical silica particles (4.82 and 1.61 μm in diameter, with a polydispersity of $<10\%$), were deposited on different substrates by means of spin coating under conditions that ensure particle isolation. For sample irradiation, an ArF excimer laser was employed to deliver single laser pulses at 193 nm, with pulse duration of 20 ns, and partial horizontal polarization, introduced by optical components in the beam path. The beam was incident normal to the sample and the intensity profile at the sample surface was designed to be top-hat, yielding homogenously illuminated circular regions with a diameter of 420 μm.[14] The irradiated regions were inspected under a commercial micro-

a)Electronic mail: j.siegel@io.cfmac.csic.es.

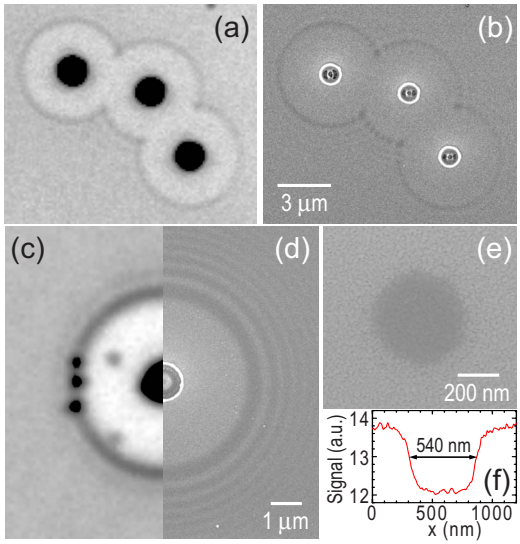

FIG. 1. (Color online) Imprints of the ONF of 193 nm light interacting with silica spheres ($\varnothing$=4.82 μm) sitting on thin fcc GST films, produced upon irradiation by single excimer laser pulses. [(a) and (b)] Imprints at low fluence (7.0 mJ/cm^2) of three spheres in close contact, measured with (a) an optical microscope (OM) and (b) a scanning electron microscope (SEM). [(c) and (d)] Imprints at slightly higher fluence (14 mJ/cm^2) of a single sphere seen with (c) OM and (d) SEM. (e) Imprint of a single sphere produced at very low fluence (0.6 mJ/cm^2), at the position of the geometric focus determined by SEM. (f) Intensity profile through (e).

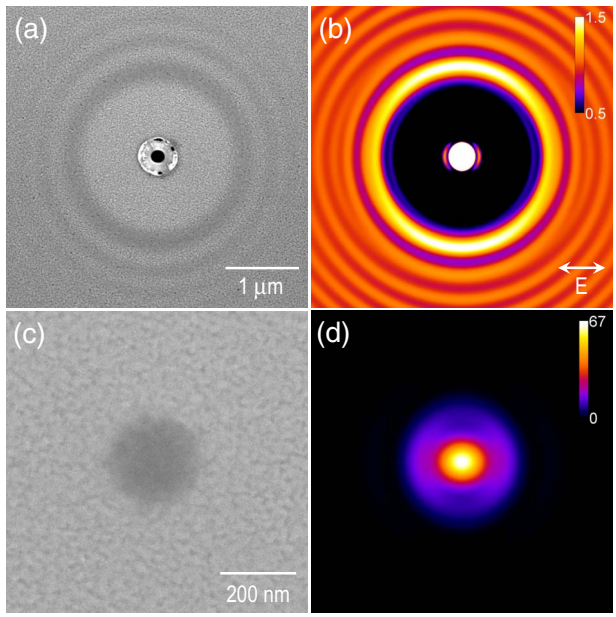

FIG. 2. (Color online) Imprints of the ONF at 193 nm using single silica spheres with $\varnothing$=1.61 μm, measured by SEM, in comparison to calculated near field intensity distributions. (a) Imprint at 13 mJ/cm^2, showing a central hole and a surrounding amorphous ring pattern. (b) Calculation corresponding to (a), zooming the intensity to display the low intensity rings. (c) Imprint at 3.5 mJ/cm^2, showing a central amorphous spot. (d) Calculated intensity distribution corresponding to (c), showing the full intensity range. The orientation of the electric field vector is along the horizontal image axis in all cases.

scope at high magnification (100×, N.A. 0.9) using light at 460 nm for illumination.

Figure 1(a) shows a region where three microspheres ($\varnothing$=4.82 μm) were initially located and removed by the laser pulse. The imprint of the ONF left behind consists essentially of three dark spots, corresponding to ablated holes at the geometric focus of the microspheres, surrounded by gray rings. These rings are a direct consequence of the interference of the incident light with the field scattered by the particle, producing a radial modulation of intensity, sufficient to trigger local amorphization in the GST film.[8] While Fig. 1(a) demonstrates how the ONF of microspheres can indeed be imprinted using UV ns laser pulses, it also illustrates the limit of OM for read-out. We have performed topographic SEM high-resolution studies performed with a Zeiss Supra 40 Field Effect Microscope, equipped with an In-lens detector for secondary electrons, at an accelerating voltage in the range of 3.5–15 kV, yielding a nominal spatial resolution of 4 nm. Figure 1(b) shows a SEM image of the same field imaged by OM in Fig. 1(a), confirming that the three central spots are ablation craters delimited by rims that appear bright in the SEM image. The amorphous rings show up gray, just as with OM. However, they are more pronounced due to the superior spatial resolution of SEM, which can be better appreciated in a direct comparison OM–SEM of an imprint produced by a single sphere [Figs. 1(c) and 1(d)]. The SEM image reveals numerous rings, whereas OM only resolves the first and in part the second ring.

We have also performed irradiation studies at very low fluence, aimed at suppressing ablation and inducing local amorphization at the geometric focus. As can be seen in the SEM image of Fig. 1(e), this can indeed be achieved, the pulse removing the particle and leaving behind an amorphous nanodot as imprint, clearly delineated from the crystalline matrix. By taking a horizontal cross section through the image center, the profile obtained [Fig. 1(f)] allows not only to determine the diameter of the nanodot (540 nm) but also to estimate the SEM signal contrast between amorphous and crystalline regions, which is about 14%.

We have performed studies also on smaller spheres ($\varnothing$=1.61 μm). Figure 2(a) shows a SEM image of an ONF imprint, which is similar to the one obtained for the larger sphere [cf. Fig. 1(d)]. We have modeled the experiment by rigorously solving Maxwell's equations for a sphere supported on a layered planar substrate,[8] assuming horizontal polarized light at normal incidence and using the optical constants of the sphere and substrate at 193 nm, except for GST, where only constants down to 240 nm were available. In particular, we have calculated the intensity distribution right underneath the GST surface (roughly proportional to the local absorption) and the result is shown in Fig. 2(b). The intensity has been zoomed to the range 0.5–1.5 (the full range being 0–67), with 1.0 referring to the intensity of the light in absence of the sphere, in order to display the low intensity interference rings surrounding the sphere. The relative intensities and positions of the experimental pattern in Fig. 2(a) are correctly predicted by the model, taking into account that high intensities induce local amorphization, which show up as dark regions in the SEM image. Even the slightly stronger contrast of the outer rings along the vertical image axis, compared to the horizontal one, can be appreciated in the experimental pattern, as predicted by the calculation.

For this smaller sphere we have also performed experiments at very low fluence, aimed at inducing local amorphization at the geometric focus. The result can be seen in the SEM image of Fig. 2(c), showing an amorphous nanodot with a diameter of $<$200 nm within a crystalline matrix. Even smaller nanodots could be produced at lower fluence,

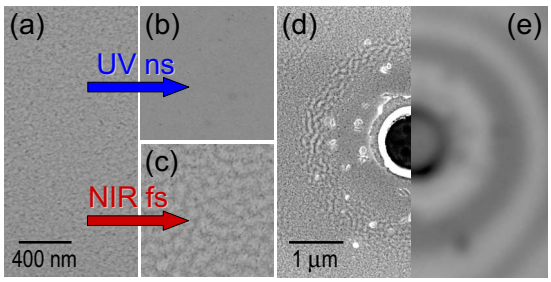

FIG. 3. (Color online) Comparison of surface morphology of GST films in different structural phases involved in laser-induced phase change. SEM images of the (a) as-grown fcc phase, (b) nanosecond-laser ($\lambda=193$ nm, $\tau=20$ ns) induced amorphous phase, and (c) fs-laser ($\lambda=800$ nm, $\tau=100$ fs) induced amorphous phase. (d) fs laser imprint of a silica sphere ($\varnothing=1.61$ μm) recorded by SEM. (e) Same as (d) but imaged by OM.

although the SEM contrast decreased correspondingly. This fluence dependence of the spot size is consistent with the threshold behavior of the material, turning amorphous over a relatively wide fluence range above threshold without causing ablation. In comparison, Fig. 2(d) shows the calculated intensity distribution, now displaying the full intensity range. The measured FWHM of the calculated distribution is $\approx$100 nm, smaller than the dot size shown in Fig. 2(c) but comparable to those obtained at smaller fluence. The somewhat larger size of the experimental dots is caused by lateral heat flow, broadening the intensity distribution and reducing the peak temperature. The characteristic diffusion length L_{th} during a laser pulse with duration τ depends on the thermal diffusivity D of the film according to $L_{th}=(D\tau)^{1/2}$. The reported value for GST is $D=0.0045$ cm^2/s,[15] yielding a diffusion length of $L_{th}=95$ nm. Although this is a relatively crude estimate, it is consistent with the difference in diameter of the amorphous nanodot and the calculated intensity distribution. We can exclude the possibility of the material being the limiting factor for achieving smaller features, since amorphous regions as small as 10 nm embedded in a crystalline film have been produced using non-laser based techniques.[16]

Finally, we have investigated the different surface morphologies of the as-grown fcc and the laser-induced amorphous phase. We have laser-amorphized a large region without particles and then recorded SEM images of it. The result is shown in Fig. 3(b), showing a much smoother surface compared to the as-grown fcc phase displayed in Fig. 3(a).

In order to compare these results to previous ones obtained using fs laser pulses,[8] we have amorphized a region without spheres using a single fs pulse ($\lambda=800$ nm, $\tau=100$ fs). The result is displayed in Fig. 3(c), showing not only a much rougher surface than the one amorphized by a UV ns laser pulse [Fig. 3(b)], but also rougher than the one of the as-grown fcc phase [Fig. 3(a)]. We attribute this roughness to the extreme conditions involved in fs laser induced amorphization, involving sharp initial temperature gradients, ultrafast melting, and extreme quenching rates. To demonstrate that this rough morphology does correspond indeed to the amorphous phase, we have performed fs laser pulse irradiation studies of a 1.61 μm sphere on GST, measuring the imprint both with SEM and OM. The result is shown in Figs. 3(d) and 3(e), unambiguously establishing that for fs laser pulses the amorphous phase (dark rings in OM) is rougher than the fcc phase (bright rings in OM), in contrast to what is observed for ns laser pulses. This finding highlights the advantage of ns laser pulses for visualizing ONFs, producing much smoother imprints.

In conclusion, we have found that ONFs produced by dielectric particles in the UV can be imaged in a simple way by imprinting the 2D intensity pattern in chalcogenide films using excimer ns laser pulses. The characteristic fingerprint consists of nanometer scale amorphous and crystalline regions that can be read out easily with high-resolution SEM. We find that thermal heat flow causes the features to fade out only slightly with respect to the incident distribution, despite the long pulse duration. In comparison, a major drawback of the use of infrared fs laser pulses has been identified to be the rough morphology of the imprints caused by the sharp initial temperature gradient, and the larger feature size related to the longer wavelength. Future work will focus on identifying the optimum pulse duration for UV light, most likely in the picosecond range, to ensure pattern smoothness and minimum feature size.

The authors thank A. Pirovano, E. Varesi, and R. Bez from Numonyx, Agrate, Italy for supplying the GST films. This project was performed within a Bilateral Agreement (2008IT0072) between CSIC (Spain) and CNR (Italy), as well as within a Joint Project between CSIC and Konstanz University, funded by the Spanish Government and DAAD. We also acknowledge partial funding from EU-FP6 Project No. NMP4-SL-2008-213669 "ENSEMBLE," Spanish national research projects (TEC2008-01183, TEC2008-03379-E, MAT2007-66050, and Consolider NanoLight.es), and by Deutsche Forschungsgemeinschaft (Grant No. SFB 513). D.P. acknowledges a grant of the Spanish Ministry of Science and Education.

[1] N. I. Zheludev, Nat. Mater. **7**, 420 (2008).
[2] P. Leiderer, J. Boneberg, V. Dobler, M. Mosbacher, H.-J. Münzer, N. Chaoui, J. Siegel, J. Solis, C. N. Afonso, T. Fourrier, G. Schrems, and D. Bäuerle, Proc. SPIE **4065**, 249 (2000).
[3] D. Brodoceanu, L. Landström, and D. Bäuerle, Appl. Phys. A: Mater. Sci. Process. **86**, 313 (2007).
[4] J. Boneberg, F. Burmeister, C. Schäfle, P. Leiderer, D. Reim, A. Fery, and S. Herminghaus, Langmuir **13**, 7080 (1997).
[5] E. McLeod and C. B. Arnold, Nat. Nanotechnol. **3**, 413 (2008).
[6] P. Hanarp, M. Käll, and D. S. Sutherland, J. Phys. Chem. B **107**, 5768 (2003).
[7] P. Leiderer, C. Bartels, J. König-Birk, M. Mosbacher, and J. Boneberg, Appl. Phys. Lett. **85**, 5370 (2004).
[8] P. Kühler, F. J. García de Abajo, J. Solis, M. Mosbacher, P. Leiderer, C. N. Afonso, and J. Siegel, Small **5**, 1825 (2009).
[9] See, for instance, the review by M. Wuttig and N. Yamada, Nat. Mater. **6**, 824 (2007).
[10] Y. Lin, M. H. Hong, T. C. Chong, C. S. Lim, G. X. Chen, L. S. Tan, Z. B. Wang, and L. P. Shi, Appl. Phys. Lett. **89**, 041108 (2006).
[11] J. Feinleib, J. deNeufville, S. C. Moss, and S. R. Ovshinsky, Appl. Phys. Lett. **18**, 254 (1971).
[12] S. R. Ovshinsky, Phys. Rev. Lett. **21**, 1450 (1968).
[13] H. F. Hamann, M. O'Boyle, Y. C. Martin, M. Rooks, and H. K. Wickramasinghe, Nat. Mater. **5**, 383 (2006).
[14] C. Dorronsoro, J. Siegel, L. Remon, and S. Marcos, Opt. Express **16**, 20955 (2008).
[15] R. Zhao, K. Lim, J. Liu, J. Ho, T. Chong, Z. Liu, B. Xu, and L. Shi, Jpn. J. Appl. Phys., Part 1 **39**, 3458 (2000).
[16] H. Satoh, K. Sugawara, and K. Tanaka, J. Appl. Phys. **99**, 024306 (2006).